Published OnlineFirst September 15, 2017; DOI: 10.1158/0008-5472.CAN-17-0496

Molecular and Cellular Pathobiology

Cancer Research

LSD1-Mediated Epigenetic Reprogramming Drives CENPE Expression and Prostate Cancer Progression

Yi Liang[1], Musaddeque Ahmed[1], Haiyang Guo[1], Fraser Soares[1], Junjie T. Hua[1,2], Shuai Gao[3], Catherine Lu[1], Christine Poon[1], Wanting Han[3], Jens Langstein[1,4], Muhammad B. Ekram[5,6,7], Brian Li[1], Elai Davicioni[8], Mandeep Takhar[8], Nicholas Erho[8], R. Jeffrey Karnes[9], Dianne Chadwick[10], Theodorus van der Kwast[11], Paul C. Boutros[2,12,13], Cheryl H. Arrowsmith[1,14], Felix Y. Feng[15,16,17,18], Anthony M. Joshua[1,19], Amina Zoubeidi[20], Changmeng Cai[3], and Housheng H. He[1,2]

Abstract

Androgen receptor (AR) signaling is a key driver of prostate cancer, and androgen-deprivation therapy (ADT) is a standard treatment for patients with advanced and metastatic disease. However, patients receiving ADT eventually develop incurable castration-resistant prostate cancer (CRPC). Here, we report that the chromatin modifier LSD1, an important regulator of AR transcriptional activity, undergoes epigenetic reprogramming in CRPC. LSD1 reprogramming in this setting activated a subset of cell-cycle genes, including CENPE, a centromere binding protein and mitotic kinesin. CENPE was regulated by the co-binding of LSD1 and AR to its promoter, which was associated with loss of RB1 in CRPC. Notably, genetic deletion or pharmacological inhibition of CENPE significantly decreases tumor growth. Our findings show how LSD1-mediated epigenetic reprogramming drives CRPC, and they offer a mechanistic rationale for its therapeutic targeting in this disease. *Cancer Res; 77(20); 5479–90. ©2017 AACR.*

[1]Princess Margaret Cancer Centre/University Health Network, Toronto, Ontario, Canada. [2]Department of Medical Biophysics, University of Toronto, Toronto, Ontario, Canada. [3]Center for Personalized Cancer Therapy, University of Massachusetts Boston, Boston, Massachusetts. [4]German Cancer Research Center, DKFZ, Heidelberg, Germany. [5]Department of Medical Oncology, The Center for Functional Cancer Epigenetics, Dana Farber Cancer Institute, Boston, Massachusetts. [6]Department of Medicine, Brigham and Women's Hospital, Boston, Massachusetts. [7]Department of Medicine, Harvard Medical School, Boston, Massachusetts. [8]Research & Development, GenomeDx Biosciences Inc., Vancouver BC, Canada. [9]Department of Urology, Mayo Clinic, Rochester, Minnesota. [10]UHN Program in BioSpecimen Sciences, Department of Pathology, University Health Network, Toronto, Ontario, Canada. [11]Department of Pathology and Laboratory Medicine, Toronto General Hospital/University Health Network, Toronto, Canada. [12]Informatics and Biocomputing Program, Ontario Institute for Cancer Research, Toronto, Ontario, Canada. [13]Department of Pharmacology and Toxicology, University of Toronto, Toronto, Ontario, Canada. [14]Structural Genomics Consortium, University of Toronto, Toronto, Ontario, Canada. [15]Department of Radiation Oncology, University of California at San Francisco, San Francisco, California. [16]Department of Urology, University of California at San Francisco, San Francisco, California. [17]Department of Medicine, University of California at San Francisco, San Francisco, California. [18]Helen Diller Family Comprehensive Cancer Center, University of California at San Francisco, San Francisco, California. [19]Kinghorn Cancer Centre, St Vincent's Hospital, Sydney, Australia. [20]Vancouver Prostate Centre, Vancouver, British Columbia, Canada.

Note: Supplementary data for this article are available at Cancer Research Online (http://cancerres.aacrjournals.org/).

Y. Liang and M. Ahmed contributed equally and share first authorship of the article.

Corresponding Author: Housheng H. He, Princess Margaret Cancer Centre, 101 College Street, PMCRT 11-305, Toronto, Ontario M5G1L7, Canada. Phone: 416-581-7736; Fax: 416-581-7736; E-mail: hansenhe@uhnresearch.ca

doi: 10.1158/0008-5472.CAN-17-0496

Introduction

Androgen receptor (AR) is highly expressed in prostate cancer cells and transactivates target genes that play essential role in tumour development and progression (1, 2). Patients with advanced and metastatic prostate cancer are typically treated with androgen-deprivation therapy (ADT) to block AR activity. Although initially effective, resistance to ADT often arises and results in castration-resistant prostate cancer (CRPC). Concordantly, AR expression is generally increased in CRPC and most AR-stimulated genes are highly expressed, indicating that *AR* transcriptional activity has been substantially restored (2). The recent clinical success of abiraterone (a CYP17A1 inhibitor that further suppresses androgen synthesis) and enzalutamide (a second-generation AR antagonist) has confirmed that AR signaling is a key driver of tumor progression in CRPC (3–5). However, these agents can only retard disease progression, and patients undergoing ADT generally relapse within 1 to 2 years. Therefore, developing novel therapeutic options are in urgent need for the treatment of CRPC patients.

Epigenetic regulators that control key epigenetic alterations, including histone modification and DNA methylation, have been recognized to play key roles in the dysfunction of transcriptional regulation in cancer cells. Among the epigenetic regulators, lysine-specific demethylase 1A (KDM1A/LSD1) is of particular interest in AR signaling. LSD1 is a histone-modifying enzyme responsible for demethylation of histone H3 lysine 4 (H3K4). Best characterized as a transcriptional repressor, LSD1 interacts with the repressive CoREST complex and demethylates enhancer-associated H3K4me1/2 (6–10). In contrast to its well-established transcriptional suppressive function, LSD1 has been reported to interact

Published OnlineFirst September 15, 2017; DOI: 10.1158/0008-5472.CAN-17-0496

with AR and function as an upstream active regulator of AR signaling in prostate cancer (11–16).

LSD1 has been characterized as a potential oncogene and a therapeutic target in several cancer types (17–19). In acute myeloid leukemia (AML), LSD1 overexpression blocks differentiation and confers a poor prognosis (20, 21). Targeting LSD1 using small-molecule inhibitors in leukemia and small cell lung cancers is efficient and the efficacy is associated with a DNA hypomethylation signature (22). LSD1 promotes proliferation of androgen-dependent prostate cancer cells (12), yet its function in CRPC remains unclear. To fill this gap, we integrated RNA-seq and ChIP-seq data to systematically assess the function of LSD1 in CRPC. We identified LSD1-mediated epigenetic reprogramming in CRPC, which activates a group of cell-cycle genes, including CENPE, to drive prostate cancer progression. Taken together, our data provide a strong rationale to target CENPE in patients with CRPC.

Materials and Methods

Cell culture and treatment

LNCaP, 22Rv1, and VCaP cell lines were obtained from the American Type Culture Collection (ATCC) in September 2013. Abl cell line was established by Dr. Helmut Klocker's laboratory (23) and obtained by the He laboratory in September 2013. Castration-resistant cell lines V16A, MR42D, and MR42F were established by Dr. Amina Zoubeidi's laboratory and obtained by the He laboratory in October 2014. All prostate cancer cell lines were cultured as recommended by ATCC or the laboratories that generated the cell lines. Regular authentication was done by short-tandem repeat profiling. Mycoplasma testing was routinely done with the MycoAlert Mycoplasma Detection Kit (LT07-118, Lonza). The most recent reauthentication and mycoplasma testing was completed in March 2017. All the cell lines were resuscitated every 3 to 4 months. LNCaP cells were androgen-starved for 48 hours followed by 4 or 24 hours DHT stimulation (10 nmol/L). CRPC cell lines, including abl and V16A cells, were cultured in androgen-deprived condition. Colony-formation assays were performed as described previously (24). Cells were synchronized by the treatment of thymidine (G_1–S phase) or nocodazole (G_2–M phase). Cell-cycle assays were performed using standard PI staining.

siRNA transfection

siRNAs targeting LSD1/KDM1A and control siRNAs were purchased from GE Dharmacon. siRNAs targeting CENPE and control siRNA were purchased from ThermoFisher. Lipofectamine RNAiMAX transfection reagent (13778150, ThermoFisher) was used for siRNA transfection following the manufacturer's instructions. All target sequences were listed in Supplementary Table S1.

CENPE overexpression

Plasmids of pCMV6-CENPE and empty vector were purchased from OriGene (Cat# RC224375 and PS100001). Lipofectamine 3000 transfection reagent (L3000015, ThermoFisher) was used for plasmid transfection following the manufacturer's instructions.

Cell-cycle analysis

Cells treated with thymidine/nocodazole or transfected with siRNA were fixed with pre-cold 70% ethanol. After fixation at −20 degrees overnight, cells were treated with 2 mg/mL RNase A solution, and incubated with 0.1 mg/mL PI solution for 30 minutes at room temperature. Data were collected on cytometer using CELLFIT and analyzed using FlowJo.

Preparation of CRISPR-Cas9 lentiviral vectors and infection

sgRNAs targeting CENPE were inserted into pLentiCRISPR vector that was generated by Dr. Zhang's lab (25). Lentiviral particle production and infection were performed as described previously (26). In brief, lentiviral vectors were cotransfected with psPAX2 and pMD2G vectors into HEK293T cells. Supernatant was collected at 24 and 48 hours after transfection and stored in −80°C. For infection, 5×10^4 cells per well were seeded in six-well plates and infected with lentiviral supernatant on the following day. The transfected cells were selected by Puromycin for 3 days. The sequences of sgRNAs targeting CENPE were listed in Supplementary Table S1.

Chromatin immunoprecipitation

Chromatin immunoprecipitation (ChIP) assay was performed using LNCaP cells treated with DHT for 24 hours or abl cells cultured under androgen-deprived condition. Protein A (88845, ThermoFisher) and G (88847, ThermoFisher) Dynabeads were mixed at a 1:1 ratio, and preincubated with antibodies 3 hours before immunoprecipitation. Cells were crosslinked by 1% formaldehyde for 10 minutes and then quenched with 125 mmol/L glycine. After cold PBS wash, nuclear fraction was extracted by 10 mL of LB1 buffer (50 mmol/L HEPES–KOH, pH 7.5; 140 mmol/L NaCl; 1 mmol/L EDTA; 10% glycerol; 0.5% IGEPAL CA-630; 0.25% Triton X-100) for 10 minutes at 4°C. Nuclear fraction was then pelleted and resuspended in 10 mL of LB2 buffer (10 mmol/L Tris–HCL, pH8.0; 200 mmol/L NaCl; 1 mmol/L EDTA; 0.5 mmol/L EGTA) at 4°C for 5 minutes. Nuclear fraction was pelleted again and resuspended in LB3 buffer (10 mmol/L Tris–HCl, pH 8; 100 mmol/L NaCl; 1 mmol/L EDTA; 0.5 mmol/L EGTA; 0.1% Na–Deoxycholate; 0.5% N-lauroylsarcosine; Protease inhibitor cocktail). Nuclear fraction was sonicated in a water bath sonicator (Diagenode bioruptor) to generate chromatin fragments at ∼300 bp. The 1/10 volume of 10% Triton X-100 was added to chromatin lysate. Chromatin lysate was cleared by centrifugation and 1/10 of supernatant was taken as input DNA. The left chromatin lysate was divided equally to antibody-conjugated beads tubes and rotated at 4°C overnight. Antibodies used for ChIP assays are LSD1 (ab17721, Abcam), AR (sc-13062, Santa Cruz Biotechnology), POLII (ab5408, Abcam), and RB1 (#9313, Cell Signaling Technology). The beads were washed by RIPA buffer and elution buffer (0.1 mol/L NaHCO3; 1% SDS; Proteinase K) was used to reverse crosslinking of DNA–protein complex at 65°C for 8 to 16 hours. DNA was purified by phenol–chloroform extraction and subjected to qPCR. All primers used in this study were listed in Supplementary Table S1.

Western blotting

Cells were lysed using RIPA buffer. Cell lysates were cleared by centrifugation (20,000× g × 10 minutes, 4°C), and the supernatant was measured by the Bio-Rad Protein Assay Kit (#5000002, Bio-Rad) according to the manufacturer's protocol. Proteins were mixed with 4× Bolt LDS Sample Buffer (B0007, ThermoFisher Scientific), and boiled for 10 minutes. Protein samples were then separated by 4% to 12% SDS-PAGE (NW04120BOX, ThermoFisher Scientific), and transferred onto PVDF membranes. The immunoreactive proteins were then visualized by ECL substrate

Published OnlineFirst September 15, 2017; DOI: 10.1158/0008-5472.CAN-17-0496

(34096, ThermoFisher Scientific). The antibodies used for Western blot were AR (sc-13062, Santa Cruz Biotechnology), LSD1 (ab17721, Abcam), GAPDH (sc-25778, Santa Cruz Biotechnology), CENPE (ab133583, Abcam), and RB1 (#9313, Cell Signaling Technology).

Tumor specimens

Fresh-frozen tissues utilized in this study were from radical prostatectomy series and from the Rapid Autopsy Program at University Health Network (UHN). For all specimens, informed consent was obtained from all subjects in accordance with the requirements of the Institutional Review Board of UHN. All patient studies were conducted in accordance with the International Ethical Guidelines for Biomedical Research Involving Human Subjects (CIOMS). Tumor specimens were obtained from the UHN Pathology BioBank and evaluated by genitourinary pathologist (T.v.d.K) on scanned, hematoxylin and eosin (H&E)-stained slides. Samples with more than 70% tumor cellularity were used for RNA extraction using the PureLink RNA Mini Kit (12183018A, ThermoFisher Scientific).

Murine prostate tumor xenograft model

Mice were anaesthetized using 2% isoflurane (inhalation) and 1×10^6 V16A prostate cancer cells suspended in 100 ml of PBS with 50% Matrigel (BD Biosciences) were implanted subcutaneously into the dorsal flank on the right side of the mice. Once the tumors reached a palpable stage ($\sim$200 mm^3), the animals were randomized and treated with vehicle (DMSO), 50 or 100 mg/kg body weight GSK923295 intraperitonially, respectively, every other day for the first 2 weeks. Growth in tumor volume was recorded using digital calipers, and tumor volumes were estimated using the formula $(\pi/6)$ $(L \times W^2)$, where L is the length of tumor and W is the width. Loss of body weight during the course of the study was also monitored. Animal survival was determined based on the tumor sizes reaching maximal volumes allowable (1,500 mm^3) under the University Health Network Institutional Animal Care and Use Committee (IACUC). At the end of the studies, mice were killed and tumors extracted and weighed. The tumor RNAs were extracted using PureLink RNA Mini Kit (12183018A, ThermoFisher Scientific). All cells planned for inoculation into mice require the authentication of being free of all *mycoplasma* contamination. Typically, qPCR profiling of mycoplasma contamination was performed prior to inoculation. All experimental procedures were approved by the University Health Network IACUC under the protocol AUP 4714.4.

RNA sequencing and gene expression analysis

LNCaP and abl cells were transfected by siRNAs targeting LSD1 or CENPE for 48 hours, and RNAs were extracted using the RNeasy Mini Kit (#74106, Qiagen) according to the manufacturer's instruction. The RNA-seq libraries were prepared using TruSeq Stranded mRNA Library Preparation Kit (RS-122-2101, Illumina) according to the manufacturer's Low Sample (LS) Protocol. Sequencing was performed at the Princess Margaret Genomic Centre. The sequencing output was aligned to Hg19 using TopHat2 version 2.1.0, and the differential expression was calculated using cuffdiff command of the Cufflinks version 2.1.1 software. The gene set enrichment analysis was made using DAVID 6.7 (27, 28). The geneset/pathway enrichment analysis has been performed using Metacore (Thomson Reuters).

The RNA-seq data for 333 primary samples and 51 benign samples were downloaded from The Cancer Genome Atlas (TCGA). The raw SRA files were downloaded for all samples from respective sources, and aligned to reference human genome version Hg19 using RSEM. The quantification of reads across the genes annotated in RefSeq was computed using DESeq2. The differential expression was calculated using negative binomial test using DESeq2. The read counts for genes were normalized for sequencing depth using DESeq2. Any gene with a fold change of 1.5 and q-value $\leq$ 0.1 is considered differentially expressed throughout the study unless otherwise specified.

ChIP-seq data analysis

The ChIP-seq libraries were prepared from ChIP DNAs using the ThruPLEX DNA-seq Kit (R400428, Rubicon Genomics) according to the manufacturer's protocol. Sequencing was performed at the Princess Margaret Genomic Centre. All ChIP-seq data were aligned against Hg19 using Bowtie2 version 2.0.5 and the peaks were called using MACS2 version 2.0.10 in its default setting. The total reads for each ChIP-seq data were subsampled to identical number when necessary to avoid bias in peak-calling due to variable sequencing depth.

Survival analysis using CENPE-induced cell-cycle genes

The normalized $\log_2$ mRNA expression data for MSKCC were obtained from cBioPortal (29). To compute the Kaplan–Meier plot using the 12 CENPE-induced cell-cycle genes for a particular dataset, we adapted a previously described strategy to assign a "risk score" to each patient based on the expression of the 12 genes (30–32). A risk score for any patient is the sum of the product of the expression value of each gene and its Cox regression coefficient. The Cox regression coefficient for each gene is determined using the Glinsky dataset (33). These coefficient values were used to compute the risk score for each patient in the TCGA dataset to perform the survival analysis. The patient group is divided into high-risk and low-risk group at the median of the risk scores. A similar analysis for metastasis and prostate cancer–specific mortality endpoints was conducted using 235 patients treated with RP at the Mayo Clinic as previously described (34). The Cox regression coefficient and the KM plots are generated using the R package "survival" version 2.40 in R version 3.2.3. The significance of the difference between two survival curves is estimated using the "survdiff" function of the aforementioned package followed by χ^2 distribution function "pchisq."

Results

LSD1 regulates different target genes in androgen-dependent and CRPC cells

To explore the role of LSD1 in the progression to CRPC, we investigated the function of LSD1 in LNCaP, the canonical androgen-dependent (AD) prostate cancer cell line, and abl, an androgen-independent derivative of LNCaP cells. LSD1 mRNA and protein expression levels in LNCaP and abl cells are similar (Fig. 1A), consistent with the observation in clinical datasets that there is no significant difference in LSD1 mRNA level between primary and metastatic CRPC tumors (Fig. 1B; Supplementary Fig. S1A). Silencing LSD1 using two independent short interfering RNAs (siRNA) targeting LSD1 reduced cell proliferation and colony growth of both LNCaP and abl

Published OnlineFirst September 15, 2017; DOI: 10.1158/0008-5472.CAN-17-0496

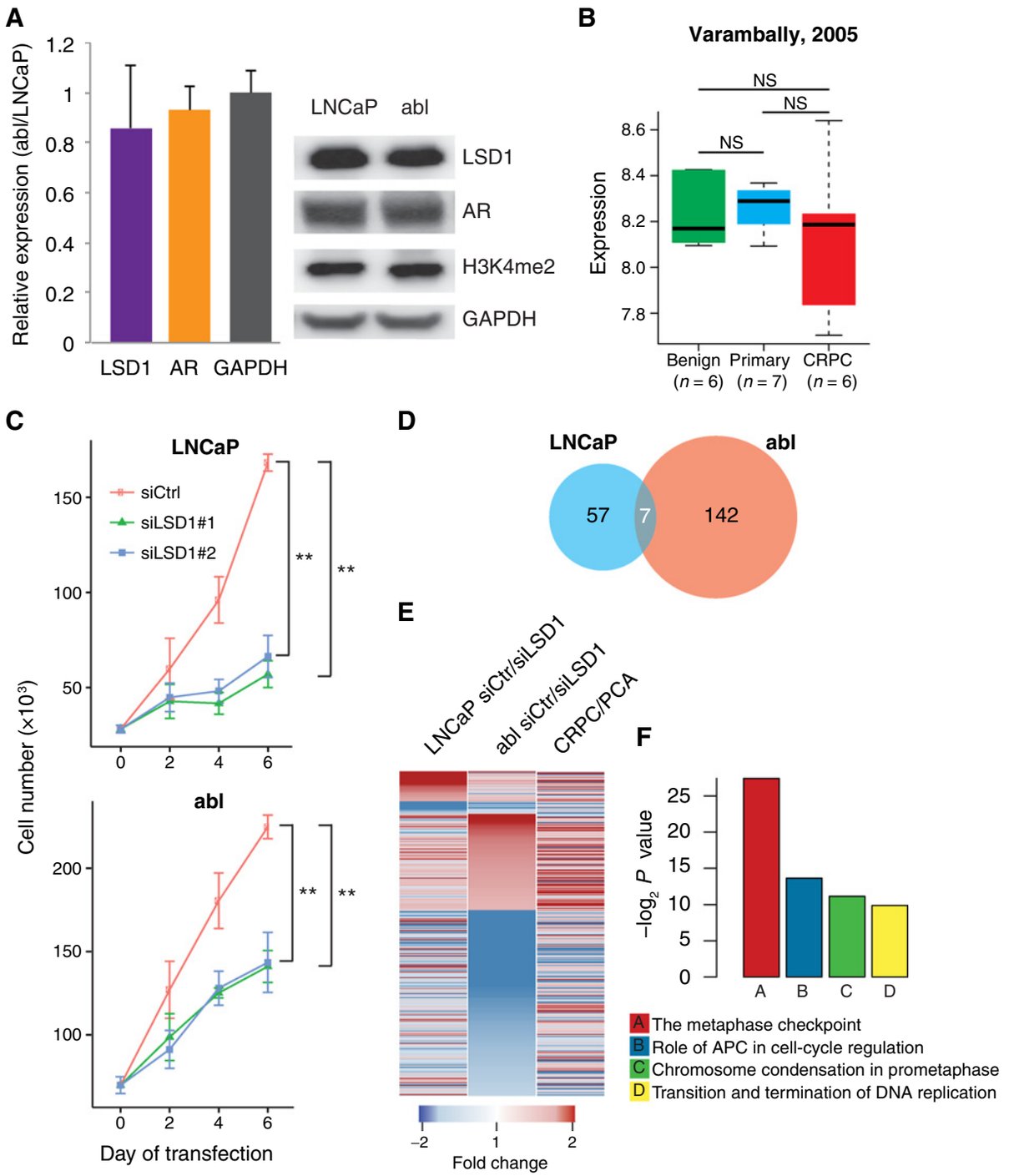

Figure 1.

LSD1 regulates prostate cancer cell proliferation and different target genes in androgen-dependent and CRPC cells. **A,** Expression of LSD1 and AR in LNCaP and abl cells. Left, the relative RNA level of LSD1 and AR in abl cells compared with LNCaP. GAPDH serves as an internal control. Data represent mean ± SD from three independent experiments. Right, the immunoblot analyses of the protein level of LSD1, AR, and H3K4me2 in the whole-cell lysate of LNCaP and abl cells. GAPDH served as a loading control. **B,** LSD1 expression level in benign prostate and prostate cancer tumor tissues from the Varambally dataset. **C,** Cell number at different time points after transfecting the LNCaP and abl cells with two independent small siRNAs targeting LSD1 and one siRNA with scrambled negative control sequence (siCtrl). Data represent mean ± SD from three replicates. **D,** Venn diagram of LSD1-induced genes in LNCaP and abl cells. **E,** LSD1-dependent genes in LNCaP and abl cells with their differential expression in metastatic CRPC compared with primary prostate cancer (PCA) tissues from Varambally dataset. **F,** The top four gene signatures enriched in genes induced by LSD1 specifically in abl cells. Gene signatures were ranked by $-\log_2 P$ value as identified in Metacore analysis. **, $P < 0.01$; NS, not significant.

Published OnlineFirst September 15, 2017; DOI: 10.1158/0008-5472.CAN-17-0496

cells (Fig. 1C; Supplementary Fig. S1B). However, when we investigated the LSD1 target genes in both LNCaP and abl cells via RNA-seq with and without silencing LSD1, we observed a large shift in LSD1 target genes (Fig. 1D; Supplementary Fig. S1C). Only 10% of genes upregulated by LSD1 in LNCaP are also upregulated by LSD1 in abl cells. Similarly, only 29% of repressed by LSD1 in LNCaP are also regulated by LSD1 in abl cells. Further, there are many more LSD1 target genes in abl compared with LNCaP cells (Fig. 1D; Supplementary Fig. S1C). When we compared the LSD1-induced genes with gene expression data in patients with metastatic CRPC or primary prostate cancer (35), we observed that these genes are generally upregulated in metastatic CRPC compared with primary tumors (Fig. 1E); however, a larger fraction of the 142 abl-specific LSD1 induced genes (80%) are upregulated in metastatic CRPC tumor than the 57 LNCaP-specific LSD1 induced genes (67%; Fig. 1E). Upon further investigation, we identified that the LSD1-induced genes in abl cells are significantly overrepresented by cell-cycle genes functioning in metaphase checkpoint, whereas the LSD1-induced genes in LNCaP cells are not (Fig. 1F; Supplementary Tables S2–S5).

These data indicate that LSD1 targets different genes in LNCaP and abl cells, although mRNA and protein levels remain largely unchanged. We therefore analyzed the genome-wide binding (cistrome) of LSD1 by performing chromatin immunoprecipitation followed by high-throughput sequencing (ChIP-seq) in both LNCaP and abl cells. Only 27% of the LSD1 binding sites in LNCaP cells are also observed in abl cells (Fig. 2A; Supplementary Fig. S2A). Furthermore, there are 8,322 genomic regions where LSD1 binds only in abl cells, but not in LNCaP cells. When we computed the association between abl-specific LSD1 regulated genes and LSD1 binding sites in both LNCaP and abl cells, we observed that the association of abl-specific LSD1-regulated genes with abl-specific LSD1 binding sites is dramatically higher than with LNCaP-specific LSD1 binding sites (Supplementary Fig. S2B and S2C). This strongly suggests that the shift in LSD1 target genes in abl is due to reprogramming of LSD1 binding.

LSD1-induced genes in CRPC are related to the prostate cancer progression

The reprogramming of LSD1 binding offers a strong premise to identify genes that are critical in progression of androgen-dependent prostate cancer to CRPC. To pinpoint such targets, we focused on the metaphase checkpoint genes that are induced by LSD1 only in abl, but not in LNCaP. Genes from the metaphase checkpoint pathway are most significantly overrepresented among the LSD1-induced genes in abl (Fig. 1F; Supplementary Table S4). There are five metaphase checkpoint genes that are induced by LSD1 specifically in abl: INCENP, BIRC5, CENPE, CENPH, and CENPA. All of these genes except CENPH are also upregulated in CRPC compared with primary prostate cancer in at least one clinical cohort (Fig. 2B). CENPE has much stronger LSD1 binding in its promoters in abl cells compared with LNCaP cells, indicating that it is upregulated directly by the LSD1 reprogramming in CRPC (Fig. 2C; Supplementary Fig. S2D–S2F). When we analyzed the binding of AR, a key driver of prostate cancer and a known interactor of LSD1 (11, 12), we observed a dramatic increase of AR binding at the CENPE promoter specifically in the abl cells (Fig. 2C). The same region also has markedly stronger enrichment of RNA Polymerase II (POLII) and H3K4me2, in abl cells compared with LNCaP cells. CENPE is significantly upregulated in CRPC compared with primary tumor in prostate cancer patients (Fig. 2B; Supplementary Fig. S3A and S3B). We extended our analysis by measuring the expression of CENPE in freshly frozen tissues from 14 and 6 prostate cancer patients with primary and CRPC tumor, respectively. The CENPE expression is more than 13 times higher in patients with CRPC tumor compared with those with primary tumor (Fig. 2D). High expression of CENPE in the primary tumor is significantly predictive of reduced disease-free survival times (Fig. 2E; Supplementary Fig. S3C and S3D). The role of CENPE in prostate cancer progression is further reflected in the clinical samples as its expression increases in tumors with increasing Gleason score (Supplementary Fig. S3E). To complement the higher expression of CENPE gene in CRPC, we measured the protein level of CENPE across seven AR-positive prostate cancer cell lines: two androgen-dependent and five androgen-independent. Consistent with the expression data, we observed that CENPE protein level is much higher in the five androgen-independent compared with the two androgen-dependent cell lines (Supplementary Fig. S3F).

LSD1 and AR coregulate the expression of CENPE by binding to its promoter region

Upon silencing LSD1 by short interfering RNA (siRNA) targeting LSD1 mRNA, we validated the efficiency of the silencing by quantifying LSD1 mRNA using RT-PCR (Fig. 3A). We then measured the expression of CENPE in both LNCaP and abl cells and observed a significant decrease of CENPE expression upon LSD1 silencing only in abl cells, but not in LNCaP cells (Fig. 3A). Consistent with the previous finding that UBE2C is selectively upregulated by AR in CRPC cells (36), we also observed that LSD1 depletes UBE2C mRNA expression selectively in abl. We validated the binding of LSD1 and AR in CENPE promoter by chromatin immunoprecipitation followed by qPCR and observed that the binding of LSD1 and AR is significantly stronger in the CENPE promoter region in abl cells compared with LNCaP cells (Fig. 3B), consistent with the LSD1 and AR ChIP-seq data (Fig. 2C). In addition, silencing of LSD1 significantly decreases AR and POLII binding, as well as H3K4me2 and H3K27ac signals at the CENPE promoter region in abl cells (Supplementary Fig. S4A and S4B). These results collectively suggest that CENPE is a direct target of LSD1 in CRPC.

As an important regulator of metaphase checkpoint, CENPE is mainly expressed at G_2–M phase during the cell cycle progression (37). To determine whether the higher level of CENPE is caused by higher percentage of cells at G_2–M phase in abl cells, we synchronized LNCaP and abl cells to G_1–S and G_2–M phases (Supplementary Fig. S5), and tested the expression of CENPE as well as the binding of LSD1/AR to the CENPE promoter region. We found that the binding of both LSD1 and AR to CENPE promoter region is significantly higher in abl compared with LNCaP, regardless of whether the cells are in G_1–S or G_2–M phase (Fig. 3C). The enrichment of POLII shows a similar trend. Consistently, the expression level of CENPE is much higher in abl cells compared with the expression in LNCaP cells regardless of cell-cycle stages (Fig. 3D). Taken together, these data support that the higher level of CENPE in CRPC is mainly due to the higher level of transcription.

Tumor suppressor retinoblastoma-associated protein 1 (*RB1*) is often lost in prostate cancer (38–40) and has recently been reported to repress transcription in presence of androgen in

Published OnlineFirst September 15, 2017; DOI: 10.1158/0008-5472.CAN-17-0496

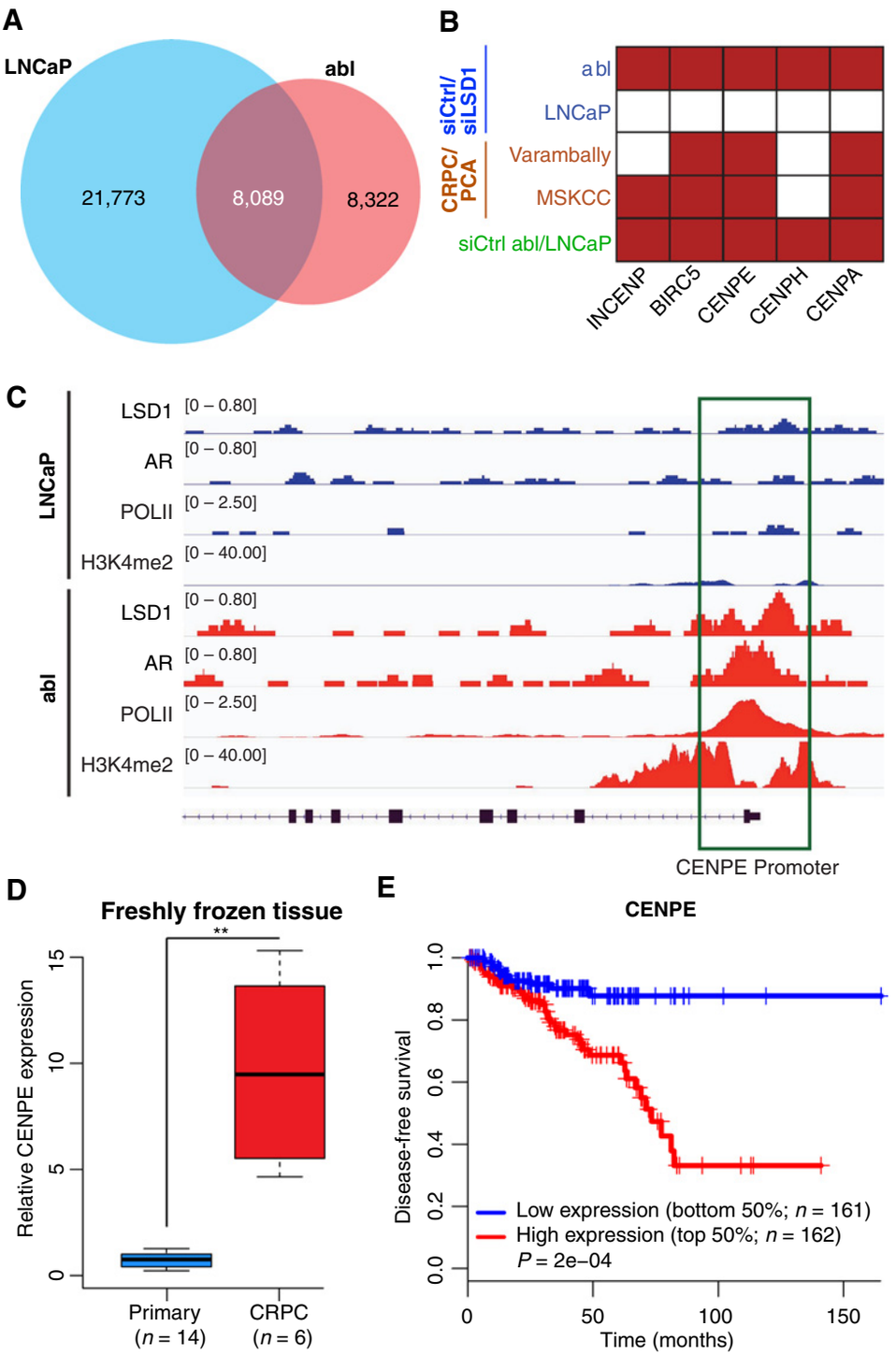

Figure 2.

CENPE is associated with the progression of prostate cancer. **A,** Venn diagram shows the overlap of LSD1 cistromes in LNCaP and abl cells. A large number of LSD1 binding sites are specific to either LNCaP or abl cells. **B,** Differential expression status of five metaphase checkpoint genes that were induced by LSD1 specifically in abl cells. Red, a significantly upregulated gene (FDR < 0.1). The first two rows indicate that these genes were induced by LSD1 in abl cells, but not in LNCaP cells. BIRC5, CENPE, and CENPA are upregulated in CRPC compared with primary prostate tumor (PCA) in two clinical datasets tested. The basal levels of all five genes were also higher in abl cells compared with LNCaP cells. **C,** The binding of LSD1, AR, POLII, and H3K4me2 on CENPE promoter region in LNCaP and abl cells. **D,** Expression level of CENPE in freshly frozen primary prostate tumor and metastatic CRPC tissues. **E,** Kaplan–Meier plot for prostate cancer patients with high or low CENPE level for disease-free survival. **, $P < 0.005$.

Published OnlineFirst September 15, 2017; DOI: 10.1158/0008-5472.CAN-17-0496

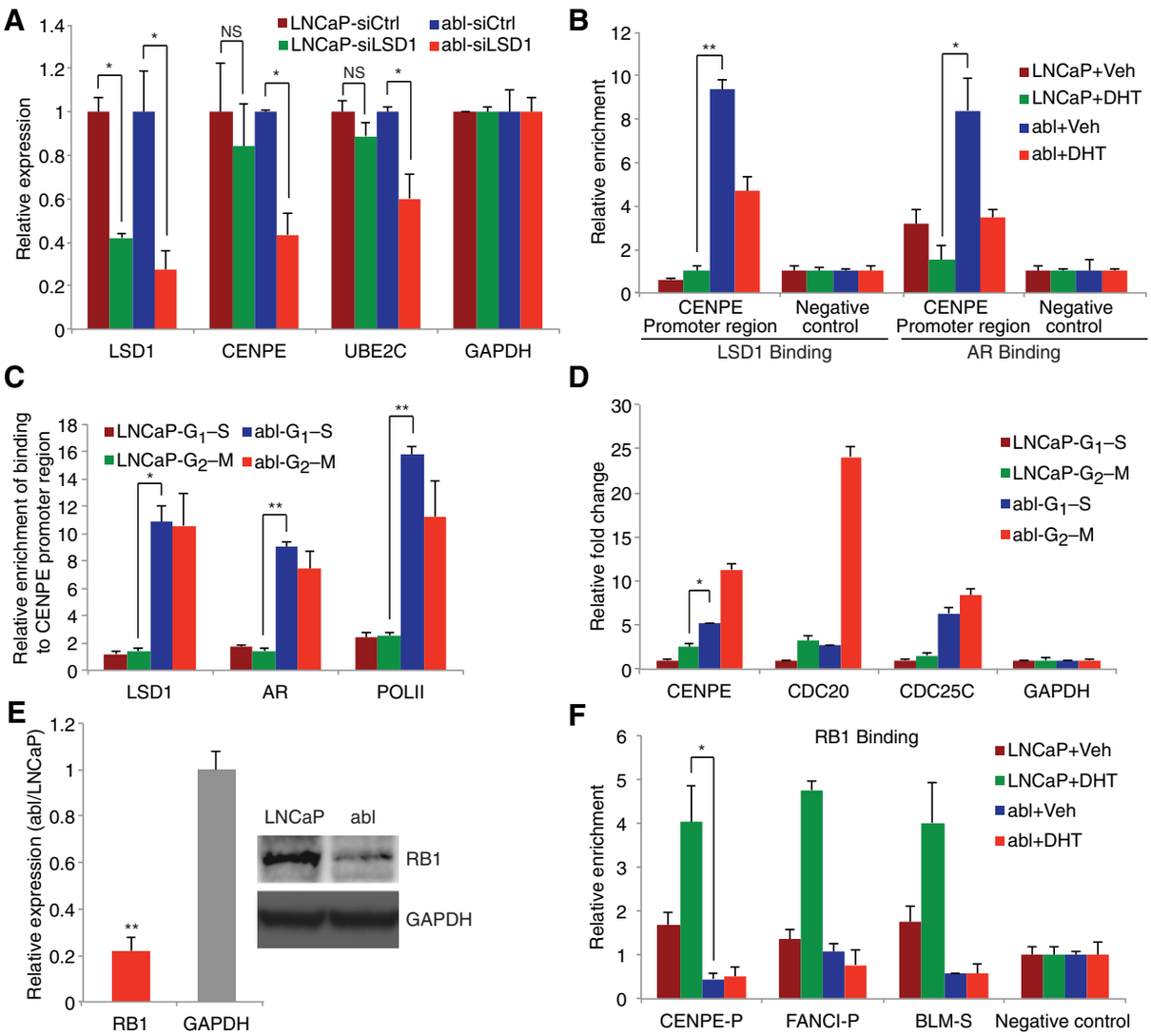

Figure 3.

LSD1 and AR coregulate the expression of CENPE by binding to its promoter region in a cell cycle-independent manner. **A,** Expression of CENPE and UBE2C after knocking down LSD1 using siRNAs in LNCaP and abl cells. The expression of LSD1 indicates good knockdown efficiency. **B,** Binding of LSD1 and AR on the promoter region of CENPE in LNCaP and abl cells with or without DHT stimulation. **C,** Binding of LSD1, AR, and POLII at the CENPE promoter region in LNCaP and abl cells arrested at different cell-cycle stages with or without DHT stimulation. **D,** Expression of LSD1-dependent genes in LNCaP and abl cells arrested at different cell-cycle stages. **E,** Quantification of RB1 mRNA and protein levels in LNCaP and abl cells. **F,** RB1 binding at the CENPE promoter region in LNCaP and abl cells with or without DHT stimulation. FANCI-P and BLM-S served as positive controls of RB1 binding (41). *, $P < 0.05$; **, $P < 0.01$; NS, not significant.

prostate cancer (41). To investigate the underlying mechanism that leads to the absence of CENPE expression in LNCaP cells, we hypothesized that RB1 could play a repressive role in controlling the LSD1/AR binding to the CENPE promoter. To test the hypothesis, we first investigated the expression of RB1 in LNCaP and abl cells; both RB1 RNA and protein levels were significantly higher in LNCaP than in abl cells (Fig. 3E). More importantly, the binding of RB1 to the CENPE promoter region in LNCaP cells stimulated by DHT is significantly stronger than that in abl cells regardless of the presence or absence of DHT (Fig. 3F). Consistently, silencing of RB1 in LNCaP cells resulted in a modest increase of LSD1 binding and a significant increase of AR binding at the CENPE promoter region, as well as a significant increase in CENPE mRNA (Supplementary Fig. S6A and S6B). These observations suggest that RB1 binds to the CENPE promoter and represses the transcription of CENPE in LNCaP cells in the presence of androgen.

CENPE regulates cell growth in CRPC specifically

From the LSD1 silencing experiments in LNCaP and abl cells, we have observed that LSD1 drives the expression of CENPE only in abl but not in LNCaP cells. Because the higher expression of CENPE is association with poor prognosis, we hypothesized that LSD1 reprogramming activates CENPE and promotes transformation of androgen-dependent prostate tumor to CRPC. This would make the oncogenic characteristic of CENPE specific to abl,

Published OnlineFirst September 15, 2017; DOI: 10.1158/0008-5472.CAN-17-0496

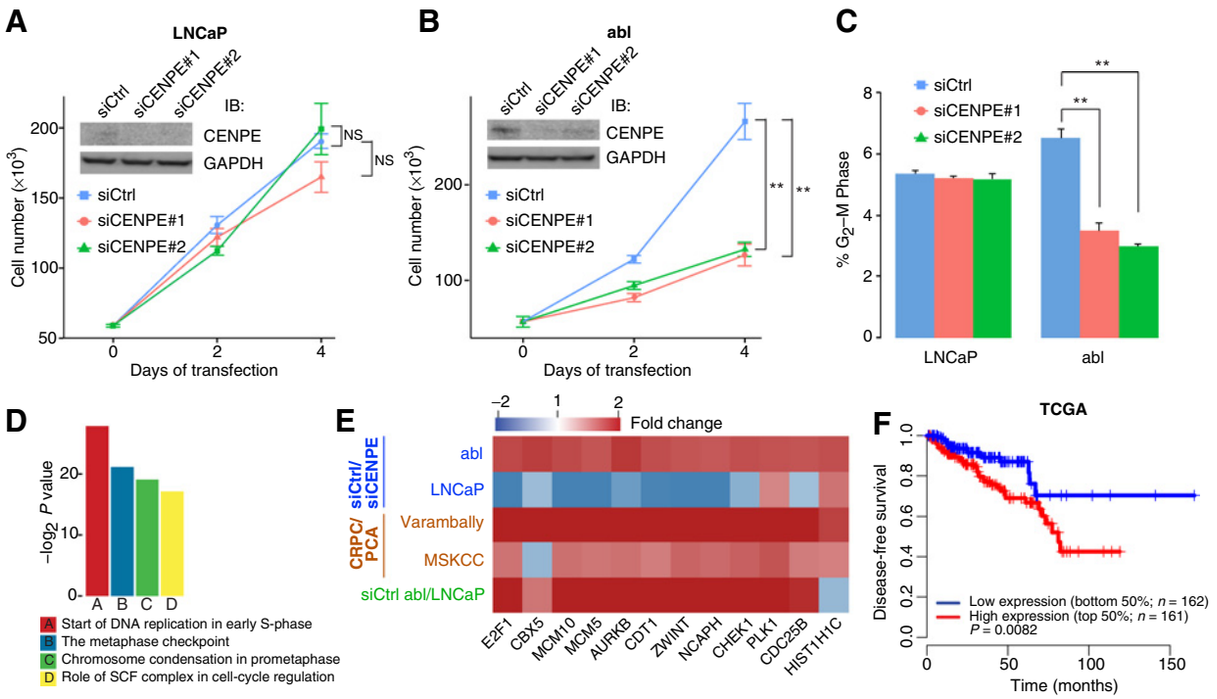

Figure 4.

CENPE regulates cell growth in CRPC specifically. **A** and **B,** Proliferation of LNCaP (**A**) and abl (**B**) cells transfected with two independent siRNAs targeting CENPE (siCENPE). Immunoblots show the knockdown efficiency. GAPDH served as a loading control. **C,** The percentage of G_2–M phase in LNCaP and abl cells after transfection with two independent siRNAs targeting CENPE. **D,** The top four CENPE-induced gene signatures in abl cells. Gene signatures were sorted by $-\log_2 P$ value as identified in Metacore analysis. **E,** Differential expression status of 12 abl-specific CENPE-induced cell-cycle–related genes in siCtrl vs. siCENPE LNCaP and abl cells, metastatic CRPC vs. primary prostate tumor (PCA) tissues from patient samples from two different cohorts and in native state (siCtrl) of abl vs. LNCaP cells. **F,** Kaplan–Meier curve for prostate cancer patients with high or low expression of CENPE-induced cell-cycle gene signature for disease-free survival. **, $P < 0.01$; NS, not significant.

not LNCaP. To test this hypothesis, we transfected both LNCaP and abl cells with two independent siRNAs targeting CENPE. Upon observing the cell proliferation for up to four days, we found that silencing CENPE significantly reduces the growth of abl cells, but the growth of LNCaP cells remains unperturbed (Fig. 4A and B). Consistently, overexpression of CENPE significantly increases growth of LNCaP cells under hormone-deprived condition (Supplementary Fig. S7A and S7B). Because CENPE is a metaphase checkpoint gene and its primary function is to drive the cells to G_2–M phase during cell cycle, we next wanted to investigate its cell cycle function in both LNCaP and abl cells. We synchronized the LNCaP and abl cells into same cell-cycle stage and treated them with two independent siRNAs targeting CENPE. After the same period of time, the fraction of siCENPE-treated abl cells in G_2–M phase is significantly lower than the abl cells treated with siRNA controls; whereas siCENPE treatment did not have any obvious effect on LNCaP cells (Fig. 4C). This indicates that the progression of abl cells to G_2–M phase is heavily dependent on CENPE, whereas the LNCaP cells do not depend on CENPE to progress to G_2–M phase.

To further investigate the selective oncogenic function of CENPE in CRPC, we performed RNA-seq of both LNCaP and abl cells upon silencing of CENPE using siRNAs. The CENPE-dependent genes are vastly different between LNCaP and abl cells. Only 4 out of the 489 CENPE upregulated genes are also upregulated in LNCaP cells (Supplementary Fig. S8A). Similarly, only 4 out of the 84 CENPE downregulated genes are also downregulated in LNCaP cells (Supplementary Fig. S8B). Metacore gene set enrichment analysis (see Materials and Methods) reveals that CENPE-induced gene sets are also completely different between LNCaP and abl cells, while the four most enriched gene sets in abl cells all cell cycle associated (Fig. 4D; Supplementary Tables S6–S9). Cell-cycle genes that are induced by CENPE in abl but not in LNCaP cells are also generally upregulated in CRPC in clinical samples, and the basal levels of these genes are also generally higher in abl than in LNCaP cells (Fig. 4E). We further investigated the potential of using these 12 CENPE target cell-cycle genes as signature marker for CRPC. We computed a risk score for each patient in multiple cohorts using the expression values of these genes (see Materials and Methods). When we generated the Kaplan–Meier plot using the clinical data and the risk scores, we observed that the higher risk score is strongly associated with poor probability of disease-free survival of the patients (Fig. 4F).

CENPE is a therapeutic target in CRPC

To test whether CENPE could serve as a therapeutic target in CRPC, we further explored the effect of disrupting CENPE using CRISPR/Cas9 approach or CENPE-specific small molecular inhibitor, GSK923295 (42) in CRPC xenografts. As abl cells are difficult to engraft, we chose V16A, an LNCaP xenograft-derived CRPC cell line for the *in vivo* analysis. V16A also has high expression of

Published OnlineFirst September 15, 2017; DOI: 10.1158/0008-5472.CAN-17-0496

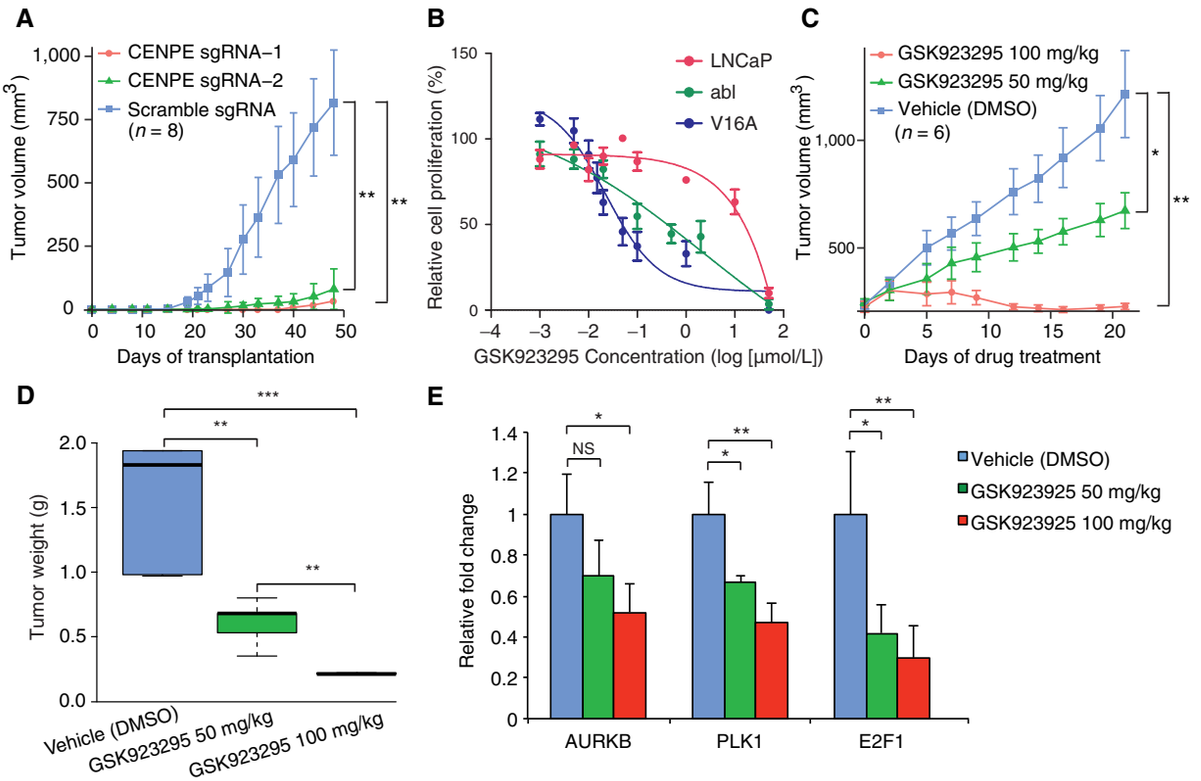

Figure 5.

Disruption of CENPE decreases tumor growth in mice. **A,** Knockdown of CENPE by the CRISPR-Cas9 system decreases tumor growth. V16A cells transfected with Cas9 as well as scrambled sgRNA and two independent sgRNAs targeting CENPE exons were implanted subcutaneously in mice ($n = 8$ per group). Caliper measurements were taken twice a week. Mean tumor volume ± SEM is shown. **B,** CENPE inhibitor GSK923295 decreases cell proliferation of CRPC cells *in vitro*. **C,** GSK923295 decreases tumor growth in a dose-dependent manner. V16A cells were implanted subcutaneously in mice and grown until tumors reached a size of approximately 200 mm^3. Xenografted mice were randomized and then administered intraperitoneally with ($n = 6$ per group) vehicle (DMSO), 50 mg/kg GSK923295, or 100 mg/kg GSK923295, as indicated, every other day for the first 2 weeks. Caliper measurements were taken twice a week. Mean tumor volume ± SEM is shown. Statistical significance was calculated by two-way ANOVA test. **D,** Tumor weight after administration of vehicle (DMSO) or two different doses of drug GSK923295. **E,** Expression of three of abl-specific CENPE-regulated cell-cycle–related genes (AURKB, PLK1, and E2F1) in tumor xenografts. *, $P < 0.05$; **, $P < 0.01$; ***, $P < 0.001$; NS, not significant.

CENPE, similar as the abl cells (Supplementary Fig. S3F). We established stable V16A cell lines with a scrambled small guide RNA (sgRNA) as well as two different sgRNAs targeting CENPE exons, following a protocol previously established (25). We found that the tumor growth of CENPE knocked-down xenografts was dramatically repressed, compared with scrambled negative control (Fig. 5A). After 7 weeks' observation, all eight mice in the scrambled sgRNA group developed tumors (100% incidence), while in the two CENPE–sgRNA groups, only one or two out of eight inoculated mice gave rise to tumors (Supplementary Fig. S9A). The mean volume of tumors in the scrambled sgRNA group was significantly higher than those of two CENPE-sgRNA groups (Supplementary Fig. S9B).

We also used GSK923295, a CENPE-specific small molecular inhibitor (42, 43), to assess the effect of small-molecule mediated CENPE inhibition on the tumor growth of V16A xenografts. First, we tested the *in vitro* cytotoxic effects in LNCaP, abl, and V16A cells and found that abl was more sensitive to CENPE inhibition than LNCaP (Fig. 5B), which is consistent with the phenotypic impact of siCENPE transfection (Fig. 4A and B). Among these three cell lines, V16A was the most sensitive one to GSK923295 (Fig. 5B). We treated V16A xenograft-bearing mice with vehicle (DMSO) or two doses of GSK923295, and observed that GSK923295 decreased tumor volume in a dose-dependent manner (Fig. 5C; Supplementary Fig. S9C). The mean tumor weight of vehicle group was dramatically higher than those of GSK923295-treated groups, and the mean tumor weight of the lower dose (50 mg/kg) group was also significantly higher compared with the 100 mg/kg group (Fig. 5D). However, GSK923295 did not significantly affect the body weight of treated mice (Supplementary Fig. S9D). Furthermore, we tested the mRNA level of three CENPE-regulated cell-cycle genes that were identified in Fig. 4E (i.e., *AURKB*, *PLK1*, and *E2F1*) and observed that the expression of these genes was repressed by GSK923295 in a dose-dependent manner (Fig. 5E). All these results support the notion that CENPE is essential to drive CRPC cell proliferation and tumor growth and could be targeted by therapeutic interventions.

Discussion

LSD1 has been previously known to be broadly associated with AR-regulated enhancers and functions as a coactivator for AR at

Published OnlineFirst September 15, 2017; DOI: 10.1158/0008-5472.CAN-17-0496

these sites (11). Epigenetic reprogramming of LSD1 in CRPC, as revealed in this study, is a novel functional role of LSD1 that can activate a set of genes functionally specific to CRPC. As a lysine-specific histone demethylase, LSD1 suppresses or activates gene expression through demethylation of H3K4me1/2 or H3K9me1/2, respectively. Recent study reported that the demethylation of H3K9me1/2 is dependent on an alternatively spliced exon of LSD1 (44). However, this isoform is not or lowly expressed in prostate cancer. How LSD1 activates gene expression in prostate cancer, especially in CRPC, is still largely unknown and warrants further study.

Our analysis showed that CENPE, a cell-cycle gene, is one of the key LSD1-induced genes in CRPC and drives the progression of prostate cancer. We observed that LSD1 and AR bind to the CENPE promoter only in CRPC, which resulted in induction of CENPE expression. CENPE is a crucial kinetochore-associated kinesin motor protein with an essential role in metaphase chromosome alignment and satisfaction of the mitotic checkpoint (37, 45, 46). CENPE is highly expressed in CRPC cell lines including abl and V16A compared with androgen-dependent prostate cancer LNCaP cells. Consistently, the level of CENPE is much higher in CRPC tumors than in primary ones. There is no significant difference of LSD1 mRNA and protein levels between androgen-dependent and CRPC cells, how LSD1 reprograms its binding to CENPE promoter and activates CENPE expression is intriguing. Interestingly, RB1, a well-characterized tumor suppressor protein, is found to bind at the CENPE promoter region in androgen-dependent prostate cancer cells but the binding is lost in CRPC cells. Consistently, silencing of RB1 in LNCaP cells resulted in increased binding of AR and LSD1 at CENPE promoter region and consequently upregulation of CENPE. This indicates that the detachment of RB1 interaction caused by loss of RB1 expression may be important for LSD1/AR transactivation activity. Further investigation is required to investigate the mechanism of how RB1 regulates the binding of AR and LSD1, i.e., how RB1 prevents the binding of AR and LSD1 at the CENPE promoter in AR-dependent prostate cancer and what triggers the loss of RB1 binding in CRPC.

While the expression of CENPE proves pivotal in driving CRPC, the gene is lowly expressed in LNCaP. Consistently, silencing CENPE has no obvious effect on the growth of LNCaP cells. The hormone-dependent prostate cancer may utilize other members of the centromere protein family to control metaphase checkpoint in the progression of the cell cycle. We observed CENPA and CENPH, two other centromere proteins, to be expressed in LNCaP cells. Interestingly, CENPH has been found to be overexpressed in many cancer types and facilitate cell-cycle progression and cell proliferation (47, 48). Nevertheless, the CRPC-biased expression of CENPE makes it an attractive therapeutic target for CRPC patients.

As an important regulator of AR transcriptional activity and as an epigenetic enzyme, LSD1 has been an attracting drug target for treatment of prostate cancer. Previous report as well as our preliminary study (data not shown) suggests that the two LSD1 inhibitors currently in clinical trials for AML and small cell lung cancer do not exhibit any cytotoxic effects on the cell proliferation of CRPC cells. However, targeting CRPC-specific LSD1-dependent genes resulting from the epigenetic reprogramming of the protein, such as CENPE, represents an alternative therapeutic measure for CRPC. Our data reveal that CENPE inhibition by small-molecule inhibitor GSK923295 significantly reduces the progression of CRPC both *in vitro* and *in vivo* in a dosage-dependent manner.

In summary, our study revealed LSD1 mediated epigenetic reprogramming as a novel mechanism in driving prostate cancer progression. LSD1-regulated CENPE may play an essential role in controlling the cell cycle and proliferation in CRPC cells specifically. Our data strongly support that CENPE can be a novel biomarker and therapeutic target for the treatment of CRPC.

Disclosure of Potential Conflicts of Interest

E. Davicioni is Chief Scientific Officer at GenomeDx. N. Erho is R&D, Manager at GenomeDx Biosciences Inc. R.J. Karnes reports receiving other commercial research support from GenomeDx and is a consultant/advisory board member for Genomic Health. F.Y. Feng is founder of PFS Genomics and is a consultant/advisory board member for Medivation/Astellas, Janssen, Dendreon, Ferring, Sanofi, and EMD Serono. No potential conflicts of interest were disclosed by the other authors.

Authors' Contributions

Conception and design: Y. Liang, M. Ahmed, H.H. He

Development of methodology: Y. Liang, M. Ahmed, H. Guo, N. Erho, H.H. He

Acquisition of data (provided animals, acquired and managed patients, provided facilities, etc.): Y. Liang, H. Guo, C. Lu, C. Poon, W. Han, J. Langstein, B. Li, E. Davicioni, R.J. Karnes, D. Chadwick, T. van der Kwast, A.M. Joshua, C. Cai, H.H. He

Analysis and interpretation of data (e.g., statistical analysis, biostatistics, computational analysis): Y. Liang, M. Ahmed, H. Guo, S. Gao, M.B. Ekram, M. Takhar, N. Erho, P.C. Boutros, C.H. Arrowsmith, F.Y. Feng, H.H. He

Writing, review, and/or revision of the manuscript: Y. Liang, M. Ahmed, H. Guo, F. Soares, J.T. Hua, S. Gao, B. Li, M. Takhar, N. Erho, R.J. Karnes, T. van der Kwast, P.C. Boutros, F.Y. Feng, A.M. Joshua, A. Zoubeidi, C. Cai, H.H. He

Administrative, technical, or material support (i.e., reporting or organizing data, constructing databases): H. Guo, J.T. Hua, E. Davicioni, C.H. Arrowsmith, H.H. He

Study supervision: H.H. He

Acknowledgments

We thank the Princess Margaret Genomic Centre for high-throughput sequencing support. The results shown here are in whole or partly based upon data generated by the TCGA Research Network.

Grant Support

This work was supported by the Princess Margaret Cancer Foundation (886012001223 to H.H. He), the Canada Foundation for Innovation and Ontario Research Fund (CFI32372 to H.H. He), NSERC discovery grant (498706 to H.H. He), WICC Ontario 20th Anniversary Prostate Cancer Innovation Grant of the CCS (703800 to H.H. He) and CIHR operating grant (142246 to H.H. He), Movember Rising Star awards (RS2014-01 to P.C. Boutros and RS2016-1022 to H.H. He) and discovery grant (D2016-1115 to H.H. He) from Prostate Cancer Canada. H.H. He holds an OMIR Early Researcher Award (ER15-11-232), a Terry Fox New Investigator Award (1069), and a CIHR New Investigator Salary Award (147820). P.C. Boutros is supported by a Terry Fox New Investigator Award, a CIHR New Investigator Award, and by the Ontario Institute for Cancer Research through funding provided by the Government of Ontario. J. Hua is a CIHR Graduate Student Fellowship recipient (GSD146249).

The costs of publication of this article were defrayed in part by the payment of page charges. This article must therefore be hereby marked *advertisement* in accordance with 18 U.S.C. Section 1734 solely to indicate this fact.

Received February 20, 2017; revised June 28, 2017; accepted August 17, 2017; published OnlineFirst September 15, 2017.

Published OnlineFirst September 15, 2017; DOI: 10.1158/0008-5472.CAN-17-0496

References

1. Green SM, Mostaghel EA, Nelson PS. Androgen action and metabolism in prostate cancer. Mol Cell Endocrinol 2012;360:3–13.
2. Yuan X, Cai C, Chen S, Chen S, Yu Z, Balk SP. Androgen receptor functions in castration-resistant prostate cancer and mechanisms of resistance to new agents targeting the androgen axis. Oncogene 2014; 33:2815–25.
3. de Bono JS, Logothetis CJ, Molina A, Fizazi K, North S, Chu L, et al. Abiraterone and increased survival in metastatic prostate cancer. N Engl J Med 2011;364:1995–2005.
4. Scher HI, Fizazi K, Saad F, Taplin ME, Sternberg CN, Miller K, et al. Increased survival with enzalutamide in prostate cancer after chemotherapy. N Engl J Med 2012;367:1187–97.
5. Ryan CJ, Smith MR, de Bono JS, Molina A, Logothetis CJ, de Souza P, et al. Abiraterone in metastatic prostate cancer without previous chemotherapy. N Engl J Med 2013;368:138–48.
6. Shi Y, Lan F, Matson C, Mulligan P, Whetstine JR, Cole PA, et al. Histone demethylation mediated by the nuclear amine oxidase homolog LSD1. Cell 2004;119:941–53.
7. Shi YJ, Matson C, Lan F, Iwase S, Baba T, Shi Y. Regulation of LSD1 histone demethylase activity by its associated factors. Mol Cell 2005;19:857–64.
8. You A, Tong JK, Grozinger CM, Schreiber SL. CoREST is an integral component of the CoREST- human histone deacetylase complex. Proc Natl Acad Sci U S A 2001;98:1454–8.
9. Lee MG, Wynder C, Cooch N, Shiekhattar R. An essential role for CoREST in nucleosomal histone 3 lysine 4 demethylation. Nature 2005;437:432–5.
10. Cai C, He HH, Chen S, Coleman I, Wang H, Fang Z, et al. Androgen receptor gene expression in prostate cancer is directly suppressed by the androgen receptor through recruitment of lysine-specific demethylase 1. Cancer Cell 2011;20:457–71.
11. Cai C, He HH, Gao S, Chen S, Yu Z, Gao Y, et al. Lysine-specific demethylase 1 has dual functions as a major regulator of androgen receptor transcriptional activity. Cell Rep 2014;9:1618–27.
12. Metzger E, Wissmann M, Yin N, Muller JM, Schneider R, Peters AH, et al. LSD1 demethylates repressive histone marks to promote androgen-receptor-dependent transcription. Nature 2005;437: 436–9.
13. Garcia-Bassets I, Kwon YS, Telese F, Prefontaine GG, Hutt KR, Cheng CS, et al. Histone methylation-dependent mechanisms impose ligand dependency for gene activation by nuclear receptors. Cell 2007; 128:505–18.
14. Barski A, Cuddapah S, Cui K, Roh TY, Schones DE, Wang Z, et al. High-resolution profiling of histone methylations in the human genome. Cell 2007;129:823–37.
15. Yatim A, Benne C, Sobhian B, Laurent-Chabalier S, Deas O, Judde JG, et al. NOTCH1 nuclear interactome reveals key regulators of its transcriptional activity and oncogenic function. Mol Cell 2012;48: 445–58.
16. Wissmann M, Yin N, Muller JM, Greschik H, Fodor BD, Jenuwein T, et al. Cooperative demethylation by JMJD2C and LSD1 promotes androgen receptor-dependent gene expression. Nat Cell Biol 2007;9: 347–53.
17. Lynch JT, Harris WJ, Somervaille TC. LSD1 inhibition: a therapeutic strategy in cancer? Expert Opin Ther Targets 2012;16:1239–49.
18. Maes T, Mascaro C, Ortega A, Lunardi S, Ciceri F, Somervaille TC, et al. KDM1 histone lysine demethylases as targets for treatments of oncological and neurodegenerative disease. Epigenomics 2015;7: 609–26.
19. Fiskus W, Sharma S, Shah B, Portier BP, Devaraj SG, Liu K, et al. Highly effective combination of LSD1 (KDM1A) antagonist and pan-histone deacetylase inhibitor against human AML cells. Leukemia 2014;28: 2155–64.
20. Harris WJ, Huang X, Lynch JT, Spencer GJ, Hitchin JR, Li Y, et al. The histone demethylase KDM1A sustains the oncogenic potential of MLL-AF9 leukemia stem cells. Cancer Cell 2012;21:473–87.
21. Schenk T, Chen WC, Gollner S, Howell L, Jin L, Hebestreit K, et al. Inhibition of the LSD1 (KDM1A) demethylase reactivates the all-trans-retinoic acid differentiation pathway in acute myeloid leukemia. Nat Med 2012;18:605–11.
22. Mohammad HP, Smitheman KN, Kamat CD, Soong D, Federowicz KE, Van Aller GS, et al. A DNA hypomethylation signature predicts antitumor activity of LSD1 inhibitors in SCLC. Cancer Cell 2015; 28:57–69.
23. Culig Z, Hoffmann J, Erdel M, Eder IE, Hobisch A, Hittmair A, et al. Switch from antagonist to agonist of the androgen receptor bicalutamide is associated with prostate tumour progression in a new model system. Br J Cancer 1999;81:242–51.
24. Liang Y, Zhong Z, Huang Y, Deng W, Cao J, Tsao G, et al. Stem-like cancer cells are inducible by increasing genomic instability in cancer cells. J Biol Chem 2010;285:4931–40.
25. Shalem O, Sanjana NE, Hartenian E, Shi X, Scott DA, Mikkelsen TS, et al. Genome-scale CRISPR-Cas9 knockout screening in human cells. Science 2014;343:84–7.
26. Guo H, Liu Z, Xu B, Hu H, Wei Z, Liu Q, et al. Chemokine receptor CXCR2 is transactivated by p53 and induces p38-mediated cellular senescence in response to DNA damage. Aging Cell 2013; 12:1110–21.
27. Huang da W, Sherman BT, Lempicki RA. Bioinformatics enrichment tools: paths toward the comprehensive functional analysis of large gene lists. Nucleic Acids Res 2009;37:1–13.
28. Huang da W, Sherman BT, Lempicki RA. Systematic and integrative analysis of large gene lists using DAVID bioinformatics resources. Nat Protoc 2009;4:44–57.
29. Cerami E, Gao J, Dogrusoz U, Gross BE, Sumer SO, Aksoy BA, et al. The cBio cancer genomics portal: an open platform for exploring multidimensional cancer genomics data. Cancer Discov 2012;2:401–4.
30. Kim SM, Leem SH, Chu IS, Park YY, Kim SC, Kim SB, et al. Sixty-five gene-based risk score classifier predicts overall survival in hepatocellular carcinoma. Hepatology 2012;55:1443–52.
31. Chen HY, Yu SL, Chen CH, Chang GC, Chen CY, Yuan A, et al. A five-gene signature and clinical outcome in non-small-cell lung cancer. N Engl J Med 2007;356:11–20.
32. Lau SK, Boutros PC, Pintilie M, Blackhall FH, Zhu CQ, Strumpf D, et al. Three-gene prognostic classifier for early-stage non small-cell lung cancer. J Clin Oncol 2007;25:5562–9.
33. Glinsky GV, Glinskii AB, Stephenson AJ, Hoffman RM, Gerald WL. Gene expression profiling predicts clinical outcome of prostate cancer. J Clin Invest 2004;113:913–23.
34. Karnes RJ, Bergstralh EJ, Davicioni E, Ghadessi M, Buerki C, Mitra AP, et al. Validation of a genomic classifier that predicts metastasis following radical prostatectomy in an at risk patient population. J Urol 2013;190:2047–53.
35. Varambally S, Yu J, Laxman B, Rhodes DR, Mehra R, Tomlins SA, et al. Integrative genomic and proteomic analysis of prostate cancer reveals signatures of metastatic progression. Cancer Cell 2005;8: 393–406.
36. Wang Q, Li W, Zhang Y, Yuan X, Xu K, Yu J, et al. Androgen receptor regulates a distinct transcription program in androgen-independent prostate cancer. Cell 2009;138:245–56.
37. Yen TJ, Li G, Schaar BT, Szilak I, Cleveland DW. CENP-E is a putative kinetochore motor that accumulates just before mitosis. Nature 1992; 359:536–9.
38. Classon M, Harlow E. The retinoblastoma tumour suppressor in development and cancer. Nat Rev Cancer 2002;2:910–7.
39. Taylor BS, Schultz N, Hieronymus H, Gopalan A, Xiao Y, Carver BS, et al. Integrative genomic profiling of human prostate cancer. Cancer Cell 2010;18:11–22.
40. Lalonde E, Ishkanian AS, Sykes J, Fraser M, Ross-Adams H, Erho N, et al. Tumour genomic and microenvironmental heterogeneity for integrated prediction of 5-year biochemical recurrence of prostate cancer: a retrospective cohort study. Lancet Oncol 2014; 15:1521–32.
41. Gao S, Gao Y, He HH, Han D, Han W, Avery A, et al. Androgen receptor tumor suppressor function is mediated by recruitment of retinoblastoma protein. Cell Rep 2016;17:966–76.
42. Qian X, McDonald A, Zhou HJ, Adams ND, Parrish CA, Duffy KJ, et al. Discovery of the first potent and selective inhibitor of centromere-associated protein E: GSK923295. ACS Med Chem Lett 2010; 1:30–4.

Published OnlineFirst September 15, 2017; DOI: 10.1158/0008-5472.CAN-17-0496

43. Wood KW, Lad L, Luo L, Qian X, Knight SD, Nevins N, et al. Antitumor activity of an allosteric inhibitor of centromere-associated protein-E. Proc Natl Acad Sci U S A 2010;107:5839–44.
44. Laurent B, Ruitu L, Murn J, Hempel K, Ferrao R, Xiang Y, et al. A specific LSD1/KDM1A isoform regulates neuronal differentiation through H3K9 demethylation. Mol Cell 2015;57:957–70.
45. Abrieu A, Kahana JA, Wood KW, Cleveland DW. CENP-E as an essential component of the mitotic checkpoint in vitro. Cell 2000; 102:817–26.
46. Wood KW, Chua P, Sutton D, Jackson JR. Centromere-associated protein E: a motor that puts the brakes on the mitotic checkpoint. Clin Cancer Res 2008;14:7588–92.
47. Liao WT, Feng Y, Li ML, Liu GL, Li MZ, Zeng MS, et al. Overexpression of centromere protein H is significantly associated with breast cancer progression and overall patient survival. Chin J Cancer 2011;30:627–37.
48. Guo XZ, Zhang G, Wang JY, Liu WL, Wang F, Dong JQ, et al. Prognostic relevance of Centromere protein H expression in esophageal carcinoma. BMC Cancer 2008;8:233.

Cancer Research
The Journal of Cancer Research (1916–1930) | The American Journal of Cancer (1931–1940)

AACR American Association for Cancer Research

LSD1-Mediated Epigenetic Reprogramming Drives CENPE Expression and Prostate Cancer Progression

Yi Liang, Musaddeque Ahmed, Haiyang Guo, et al.

Cancer Res 2017;77:5479-5490. Published OnlineFirst September 15, 2017.